

# AN ADAPTIVE MULTI-POPULATION EVOLUTIONARY ALGORITHM FOR CONTAMINATION SOURCE IDENTIFICATION IN WATER DISTRIBUTION SYSTEMS

Changhe Li<sup>1</sup>, Rui Yang<sup>2</sup>, Li Zhou<sup>3</sup>, Sanyou Zeng<sup>4</sup>, Michalis Mavrovouniotis<sup>5</sup>, Ming Yang<sup>6</sup>,  
Shengxiang Yang<sup>7</sup>, and Min Wu<sup>8</sup>

<sup>1</sup>Professor, School of Automation, China University of Geosciences, Wuhan 430074, China;  
and Hubei Key Laboratory of Advanced Control and Intelligent Automation for Complex  
Systems, Wuhan 430074, China(corresponding author). Email: changhe.lw@gmail.com

<sup>2</sup>School of Automation, China University of Geosciences, Wuhan 430074, China. Email:  
2280920465@qq.com

<sup>3</sup>School of Automation, China University of Geosciences, Wuhan 430074, China. Email:  
441837060@qq.com

<sup>4</sup>Professor, School of Mechanical Engineering and Electronic Information, China University  
of Geosciences, Wuhan 430074, China. Email: sanyouzeng@gmail.com

<sup>5</sup>KIOS Research and Innovation Center of Excellence, Department of Electrical and  
Computer Engineering, University of Cyprus, Nicosia, Cyprus. Email:  
mavrovouniotis.michalis@ucy.ac.cy

<sup>6</sup>Associate Professor, School of Computer Science, China University of Geosciences, Wuhan  
430074, China. Email: mingyang@cug.edu.cn

<sup>7</sup>Centre for Computational Intelligence (CCI), School of Computer Science and  
Informatics, De Montfort University, Leicester LE1 9BH, U. K. Email: syang@dmu.ac.uk

<sup>8</sup>Professor, School of Automation, China University of Geosciences, Wuhan 430074, China;  
and Hubei Key Laboratory of Advanced Control and Intelligent Automation for Complex  
Systems, Wuhan 430074, China. Email: wumin@cug.edu.cn

## ABSTRACT

Real-time monitoring of drinking water in a water distribution system (WDS) can effectively warn and reduce safety risks. One of the challenges is to identify the contamination source through these observed data due to the real-time, non-uniqueness, and large scale characteristics. To address the real-time and non-uniqueness challenges, we propose an adaptive multi-population evolutionary optimization algorithm to determine the real-time characteristics of contamination sources, where each population aims to locate and track a different global optimum. The algorithm adaptively adjusts the number of populations using a feed-back learning mechanism. To effectively locate an optimal solution for a population, a co-evolutionary strategy is used to identify the location and the injection profile separately. Experimental results on three WDS networks show that the proposed algorithm is competitive in comparison with three other state-of-the-art evolutionary algorithms.

**Keywords:** Multi-population adaptation, dynamic bilevel optimization, evolutionary computation, contamination source identification

## 1 INTRODUCTION

2 Water distribution systems (WDSs) are highly susceptible to various threat attempts, in-  
3 cluding uncertain natural disasters, deliberate destruction, and system failures. For example,  
4 a contamination source injected into a WDS will spread through the system rapidly and ex-  
5 pose the people to health risks. Detection of the contamination in a WDS using sensors could  
6 yield useful observations to identify and locate such contamination threat events. Based on  
7 these observations, we can deduce the location, initiation time, and historical injection rate  
8 by solving an inverse problem with an optimization algorithm given the observation data  
9 under a water distribution simulation model. Because of the rapid diffusion of contaminants  
10 in a WDS, we should identify the source characterizations quickly and accurately.

11 The problem is challenging due to the real-time, non-uniqueness/multi-modal, large-  
12 scale, and expensive characteristics. The real-time property requires the search to be data-  
13 driven, i.e., the search starts immediately after the contamination is detected at any sensor,

14 and continuously adapts to changes when new observation data come. The non-uniqueness  
15 means that more than one solutions conform to the observation data, which requires the  
16 algorithm to have the capability of searching more than one solution simultaneously. The  
17 large scale property means that the search space will increase exponentially due to the  
18 increase of the number of dimensions of the vector of the injection rate as observation data  
19 increase. The problem will become expensive to simulate when the scale of the network  
20 increases. There are mainly three kinds of methods for the identification of contamination  
21 source in WDSs, including the particle inversion method (Zierolf et al. 1998; Laird et al.  
22 2005; Shang et al. 2002; Costa et al. 2013), the machine learning method (Perelman and  
23 Ostfeld 2013; Taormina and Galelli 2018; Huang and Mcbean 2009; Yang et al. 2011), and  
24 the simulation-optimization method (Guan et al. 2006; Liu et al. 2008; Seth et al. 2016; Hu  
25 et al. 2015). The first two methods can only deduce the location of the contamination source,  
26 while the third method can deduce all the information of a contamination event. Therefore,  
27 the simulation-optimization method is adopted in this paper.

28 To address the real-time and non-uniqueness challenges, we propose a new adaptive multi-  
29 population evolutionary algorithm where the water distribution network model is coupled  
30 directly with a dynamic bilevel optimization model to evaluate solutions as new observa-  
31 tion data come. To address the non-uniqueness difficulty, we incorporate a multi-population  
32 method where each population aims to locate a different solution, and the number of pop-  
33 ulations is adaptively adjusted to adapt to the increase of observation data by a feed-back  
34 learning mechanism and hence to identify alternative solutions as many as possible. The  
35 population diversity across all network nodes will be adaptively increased according to the  
36 evolving state of populations measured by a node covering ratio. Thus, at any stage of the  
37 observation event, possible solutions that best conform to the observations are identified.  
38 In order to speed up the search for a possible solution, in each population, a cooperative  
39 co-evolutionary strategy is proposed to locate the location and historical injection rate sep-  
40 arately. Experiments in this paper are based on an EPANET 2.0 model (Rossman 2000) of

41 the water distribution network. Experimental results on three different networks show that  
42 the proposed algorithm outperforms several other peer algorithms.

43 The rest of this paper is organized as follows. Section 2 briefly reviews the related  
44 work. Section 3 presents a simulation-optimization model for the problem and introduces  
45 our proposed method. Section 4 presents experimental results on three networks. Finally,  
46 conclusions and future work are given in Section 5.

## 47 RELATED WORK

48 In this section, we focus on the review of simulation-optimization methods, which can be  
49 classified into three categories according to the optimization method used. These algorithms  
50 include the gradient descent (GD) method, the particle swarm optimization (PSO) , and the  
51 genetic algorithm (GA).

52 The basic idea of a GD method is to use the gradient direction of the current position as  
53 the search direction. Guan et al. (2006) adopted the gradient descent method as the search  
54 operator to solve the problem of locating pipe network contamination sources based on the  
55 simulation-optimization model. Xin et al. (2013) got the locally optimal solution according  
56 to the direction of gradient descent search. In this method, when approaching the optimal  
57 value, the convergence speed will gradually slow down, that is, the closer to the objective  
58 value, the step length will be smaller, and even causes a zigzag drop.

59 The genetic algorithm is based on the Darwinian evolution of “survival of the fittest”. In  
60 the literature, several papers (Preis and Ostfeld 2008; Preis and Ostfeld 2006; Sreepathi et al.  
61 2007) used GAs to solve the problem and achieved promising results. Cristo et al. (2008),  
62 firstly established the potential node-set representing the solution of pollution sources – water  
63 contamination matrix, then used a GA to search the optimal solution. Yan et al. (2016) used  
64 a hybrid encoding method to code the contaminant source identification problem according  
65 to the properties of a variable, and combined the crossover and mutation operations. Sankary  
66 et al. (2018) proposed a framework to obtain monitoring data by placing mobile sensors using  
67 an adaptive GA.

68 The PSO, which is a swarm intelligence method, originated from the study of the flocking  
69 behavior of birds simulating their behavior of flying and foraging in groups. Guneshwor et  
70 al. (2018) proposed a simulation-optimization model by using a radial point collocation  
71 method and the PSO to identify the unknown groundwater contaminant sources. In this  
72 method, due to the lack of dynamic adjustment of particle velocity, it is easy to fall into  
73 local optima. Besides the above search algorithms, an evolution strategy algorithm based on  
74 a Gaussian mutation operator (GD-ES) was proposed to generate new individuals (Zechman  
75 and Ranjithan 2009), and an elite graduation selection strategy was introduced to determine  
76 the offspring.

77 From 2008 to 2011, Liu et al. (2008, 2010, 2011) proposed a multi-population method  
78 with GA, which uses an adaptive dynamic optimization technology (ADOT) to make a  
79 real-time response to injection events to locate contamination sources. To overcome the  
80 premature convergence issue, the algorithm (Liu and Ranjithan 2010) starts with a large  
81 number of randomly generated populations and removes populations that are close to each  
82 other during the optimization process. A diversity-driven mechanism is used to increase the  
83 population diversity for the survival selection in the later evolution stage. The algorithm  
84 achieves a great performance in comparison with other optimization algorithms, but it still  
85 lacks the mechanism to search the spaces that are not covered by any population at the  
86 global level. The number of populations only decreases as time goes on. This issue will be  
87 addressed in this paper.

88 In addition to the literature on contamination source identification described above, there  
89 are some important studies on the use of evolutionary algorithms to determine the optimal  
90 locations of sensors and the developing an early warning system. Ostfeld and Salomons  
91 (2004) presented a method for finding the optimal layout of an early warning detection  
92 system. In the next year, Ostfeld and Salomons (2005) extended their previous work by  
93 a introducing uncertainties to the demands and injected contamination events. Berry et  
94 al. (2006) introduced a mixed-integer programming method for sensor placement. In the

95 same year, Propato (2006) formulated a mixed-integer linear programming model to identify  
 96 optimal sensor locations for early warning against accidental and intentional contaminations.  
 97 Olikar and Ostfeld (2014) improved the event-detection ability by including the support  
 98 vector machine for the detection of outliers and a multivariate analysis for examining the  
 99 relationship between water-quality parameters and their mutual patterns.

## 100 METHODOLOGY

101 An inverse problem can be constructed to identify the contamination source character-  
 102 istics, where the input is a set of concentration observations at sensors and the objective is  
 103 to minimize the error between predicted concentration and actual observation at sensors on  
 104 the network using a water distribution simulation model.

### 105 Simulation-optimization Model

106 The simulation-optimization model has two sub-models: a simulation model and an  
 107 optimization model. The simulation model mainly describes the water movement in a WDS,  
 108 including the water flow model and the solute transport model. The optimization model  
 109 can transform the problem into an optimization problem of describing the location of the  
 110 contamination source, the injection start time, and the injection history information.

The water flow model and water quality model in urban common water supply network can be realized by the hydraulic simulation function of water quality in EPANET 2.0. The model can simulate the diffusion of solutes in contamination events and feedback of node concentration data. We define

$$y_j(t) = \mu(\mathbf{x}(t)), j = 1, \dots, K \quad (1)$$

111 where  $y_j(t)$  denotes the concentration data of contaminants detected by sensor  $j$  at time  
 112 step  $t$  (each sensor is set at a different node);  $\mathbf{x}(t) = (x_u, \mathbf{x}_l(t))$  denotes information of a  
 113 contamination event at a single source at time step  $t$ ,  $x_u \in \mathbb{N}$  denotes the location of the  
 114 contamination source;  $\mathbf{x}_l(t) = (x_0, x_{x_0}, x_{x_0+1}, \dots, x_t) \in \mathbb{R}^{t-x_0+2}$  denotes the injection profile,

115 where  $x_0$  is the starting time and  $(x_{x_0}, x_{x_0+1}, \dots, x_t)$  is a time series of injection rate from  
 116  $x_0$  to  $t$ ;  $\mu$  is a simulation model of water distribution systems with the input  $\mathbf{x}(t)$  and the  
 117 observed output  $\mathbf{y}(t)$  of  $K$  sensors.

118 Given the water quality hydraulic simulation model, the problem of locating and tracing  
 119 contamination sources can be converted into a dynamic bilevel optimization problem. The  
 120 upper-level optimization task is to find the location ( $x_u$ ) of a contamination event, and the  
 121 lower-level task is to find the injection history profile ( $\mathbf{x}_l(t)$ ), which is defined as a dynamic  
 122 optimization problem whose variables will increase as time goes on. Note that, the problem  
 123 is defined as a single-level optimization problem in previous work discussed in Section 2.  
 124 In our experiments, we found that the location variable has a significant influence on the  
 125 distribution of the objective value and the injection profile variables do not. Therefore, we  
 126 divide the problem into two levels and solve them cooperatively.

In this paper, the square root of the mean squared error between the observed data of  
 a possible solution and the actual observed data of contamination sources is used as the  
 objective, which is shown below:

$$\begin{aligned}
 \min_{x_u, \mathbf{x}_l(t)} \quad & f_u(x_u, \mathbf{x}_l(t)) = \sqrt{\frac{\sum_{j=1}^K \sum_{s=0}^t [y_j(s) - \tilde{y}_j(s)]^2}{K \cdot t}} \\
 \text{s.t.} \quad & \mathbf{x}_l(t) \in \arg \min_{\mathbf{x}_l(t)} \{f_l(x_u, \mathbf{x}_l(t))\}
 \end{aligned} \tag{2}$$

127 where  $\tilde{y}_j(s)$  denotes the observed data at sensor  $j$  at time step  $s$  of the actual contamination  
 128 source. Therefore, the objective is to minimize the cumulated error over all sensors so far  
 129 since the initial observed data are obtained, i.e., to find a solution that complies with the  
 130 actual observation data. The two levels of problems all aim to minimize the prediction error  
 131 but have different tasks. In this paper, we solve the problem in an online manner under a  
 132 real-world scenario.

133 As mentioned above, the problem is difficult due to the real-time, non-uniqueness, large  
 134 scale, and expensive properties. For a typical WDS, the number of sensors is far less than the

135 number of nodes in the network due to the cost reason, which leads to the incompleteness  
136 of the observation data and causes many global optima of Eq. (2) at a time during the  
137 optimization process. It is a typical multi-modal optimization problem, and hence, multi-  
138 modal optimization techniques are needed to find as many global optima as possible for  
139 decision-makers to decide the actual one.

140 For the real-time property, the contamination source identification needs to start once  
141 contaminants are detected immediately. With the increase of the observation data, the input  
142 of the objective function will continuously change, which may cause the optimal solution set  
143 to change. Therefore, it is necessary to identify the optimal solution location in real-time  
144 when solving the problem, that is, to solve the problem with dynamic optimization method,  
145 to ensure that the source information can be obtained in time when the contamination event  
146 occurs.

147 The large-scale property couples with the expensive property. There are mainly three  
148 aspects to be considered. Firstly, when the scale of a WDS is quite large, the simulation  
149 time of evaluating a solution will become unaffordable (i.e., it becomes expensive), and the  
150 value range of the location of  $x_u$  will be increased sharply, resulting in a sharp increase in  
151 solution space. Secondly, the dimension for historical contamination injection rate of  $\mathbf{x}_l$  will  
152 increase as the contamination event keeps on. As the dimension of  $\mathbf{x}_l$  increases linearly,  
153 the solution space increases exponentially, which makes it challenging for an algorithm to  
154 find the optimal solution. Thirdly, when multiple contamination sources exist, the solution  
155 representation becomes multiple time series, which makes the problem much more difficult  
156 to solve.

157 In this paper, we mainly focus on addressing the former two considerations in a network  
158 with a single contamination source. To address them, we propose an adaptive multiple  
159 population framework to find multiple global solutions and adaptively adjust the number of  
160 populations to adapt to the changes in observed data.



## 161 **Adaptive Multi-population Algorithm**

162 Multi-population (MP) methods are very efficient for tracking and locating multiple  
163 optima in dynamic environments. This section presents the details of the adaptive multi-  
164 population (AMP) framework proposed in this paper.

### 165 *Algorithm Framework*

166 The framework has three basic components: clustering, parallel search, and diversity  
167 increasing components. Figure 1 shows the framework, where  $m$  is the size of a population  
168 (fixed in the paper),  $k(T)$  is the total number of populations at time  $T$  (a counter that keeps  
169 the number of times the diversity increasing component is triggered after clustering),  $\tilde{k}(T)$   
170 is the number of populations survived after the parallel searching, and  $\Delta k(T)$  is the number  
171 of population to be added.

172 Algorithm 1 presents the pseudo-code of the framework of the adaptive multi-population  
173 algorithm. The framework starts with a set of randomly initialized individuals at  $T=0$ , then  
174 clusters these new individuals to a set of populations. Populations simultaneously search for  
175 global optima and merge if their best individuals locate at the same node on the network.  
176 When the coverage ratio over all nodes does not change over two successive generations, it  
177 will trigger the diversity increasing procedure where a feedback learning method is used to  
178 control the number of populations to be added.

### 179 *Generation of Multiple Populations*

180 The idea of *divide-and-conquer* is adapted to make each population search for different  
181 regions, which is equivalent to reducing the search area of each population. For this purpose,  
182 the  $k$ -means clustering method is adopted in this paper to generate multiple populations  
183 whose search areas are not overlapping with each other.

We firstly generate a certain number of individuals at node  $i$  with a probability  $p_i$ , which  
is the same ( $p_i = 1/n$ ,  $n$  is the number of nodes of a network) for all nodes at the beginning

---

**Algorithm 1:** Pseudo-code of the adaptive multi-population framework

---

```
Set  $T \leftarrow 0$ ;  
Randomly initialize  $k(T) * m$  solutions;  
while new observation data are detected do  
    Clustering newly generated solutions;  
    while coverage ratio changes do  
        Cooperatively co-evolve each population by GL (Xia and Li 2016) and  
        SaDE (Qin et al. 2009) for one iteration;  
        if the best solutions of more than one population cover the same node then  
            Merge these populations by the competition mechanism;  
        Update the coverage ratio on the whole network;  
    Update the node selection probability by Eq. (3);  
    Estimate the number of populations ( $\Delta k(T)$ ) to be increased by Eq. (5);  
    Generate  $\Delta k(T) \cdot m$  solutions on the network according to the probability  
    obtained by Eq. (3);  
     $T \leftarrow T + 1$ ;
```

---

of a run and is updated before the increase of populations by:

$$p_i(T) = 1 - \frac{\sum_{s=0}^T \kappa_i(s)}{\max_{i \in n} \sum_{s=0}^T \kappa_i(s)} \quad (3)$$

184 where  $\kappa_i(s)$  is the accumulated times of node  $i$  visited by individuals since the start of the run.  
185 From Eq. (3), we can see that the more times a node is visited, the smaller the probability  
186 of being selected when generating new solutions. For example, if a node has never been  
187 visited by any individuals, the probability of being chosen will be one when generating new  
188 solutions.

189 After that, the nodes covered by all new individuals are then clustered by the  $k$ -means  
190 clustering method. Algorithm 2 shows the procedures of the  $k$ -means clustering method,  
191 where the estimation of the number of clusters  $\Delta k(T)$  to be clustered will be given later  
192 in Section 3. Eventually, individuals of a cluster consist of a new population. Note that  
193 the shortest distance of two nodes across the network can be used instead of the Euclidean  
194 distance used in this paper.

---

**Algorithm 2:** Pseudo-code of the  $k$ -means clustering

---

```
Initialize  $\Delta k$  cluster centers;  
while clusters do not converge, i.e., cluster centers are still changing do  
  for each node do  
    Calculate the Euclidean distance from the node to each cluster center;  
    The node is assigned to the cluster whose center is nearest to the node;  
  Recalculate the center of each cluster;
```

---

195 *Cooperative Co-evolutionary Search*

196 The representation of the solution to the problem is composed of discrete and continuous  
197 parts. The location variable is an integer, and the injection profile is represented by a vector  
198 of real values. To alleviate the difficulty in searching the solution of the hybrid representation,  
199 we use the cooperative co-evolution (CC) strategy (Potter and De Jong 1994) to solve the  
200 upper-level and lower-level problems separately.

201 *Cooperative Co-evolution*

202 Cooperative co-evolution (Potter and De Jong 1994; Yang et al. 2017) is an extension of  
203 the traditional evolutionary algorithm inspired by the strategy of *divide-and-conquer* when  
204 dealing with large scale optimization problems. By decomposing decision variables into a  
205 set of independent groups (each group of variables consists of a subproblem), the original  
206 problem can be solved by solving these subproblems by different algorithms. We use two  
207 different single-population based algorithms to solve the two levels problems using the CC  
208 strategy, i.e., when evaluating a solution in one population, the value of the remaining  
209 information is taken from the best solution of the other population.

210 *Genetic Learning*

211 Genetic learning (GL) (Xia and Li 2016) is an optimization method based on probability  
212 and statistics. It consists of two components: gene prediction and gene exploration. The  
213 gene prediction uses a probability model build on historical data to select genes, and the  
214 gene exploration attempts to discover new genes to increase the population diversity. These  
215 two components interact to form a feedback system. The genetic learning method makes

---

**Algorithm 3:** Pseudo-code of the genetics learning algorithm

---

```
for each individual do  
     $idx \leftarrow$  node index of the current individual;  
     $obj \leftarrow$  prediction error of the current individual;  
     $sum\_obj_{idx} \leftarrow sum\_obj_{idx} + obj$ ;  
     $count_{idx} \leftarrow count_{idx} + 1$ ;
```

---

216 full use of the historical information generated in the iteration process. It analyses the  
217 fitness of each individual in every possible value of each decision variable and calculates the  
218 probability of each value being selected. It then performs the mutation operation in each  
219 dimension according to these probabilities.

We use this method to find the injection location of the upper-level problem. For each population, we count the cumulative prediction objective value  $sum\_obj$  of each node in the network. Algorithm 3 shows the specific steps. The probability of node  $idx$  to be selected can be obtained by:

$$p_{idx} = \frac{mean_{max} - mean_{idx}}{\sum_{i=1}^n mean_{max} - mean_{idx}} \quad (4)$$

220 where  $mean_{idx} = sum\_obj_{idx}/count_{idx}$ ,  $mean_{max} = \max(mean_i \mid i = 1, 2, \dots, n)$ . The  
221 probability will be updated every iteration. The nodes with smaller errors have larger prob-  
222 abilities to be selected for GL.

### 223 *Strategy Adaptation Differential Evolution*

224 Differential evolution (DE) (Storn and Price 1997) is a simple yet effective optimization  
225 algorithm, especially for solving continuous optimization problems. The strategy adaptive  
226 differential evolution algorithm (SaDE) (Qin et al. 2009) is an enhanced version, where  
227 the differential operators are selected adaptively according to their performance in previous  
228 generations. Here four classical difference operators  $DE/rand/1$ ,  $DE/best/1$ ,  $DE/target-to-$   
229  $best/1$  and  $DE/best/2$  are used to optimize the initial time and historical injection rate.  
230 Note that the recommended values for parameters of SaDE (Qin et al. 2009) were used in  
231 this paper.

### 232 *Population Management*

233 Population removal and population increase are two critical components of the adaptive  
234 multi-population framework, especially in dynamic environments (Yang and Li 2010; Li and  
235 Yang 2012; Li et al. 2015). The population removal component aims to remove redundant  
236 populations, and hence to save computational resources. The population increase component  
237 aims to increase the diversity in the areas which have not been searched or not sufficiently  
238 searched so far, and hence to find more global optima solutions.

### 239 *Population Removal*

240 After the clustering, each population will cover a unique search area containing one or  
241 several geographically closed nodes on the network. As the search goes on, some of the  
242 populations may move toward the same area, and finally, converge at the same node of that  
243 area. This causes redundant search, which should be prevented. To prevent more than  
244 one population from searching in the same area, we check their best solutions. When their  
245 best solutions locate at the same node on the network, these populations are deemed to be  
246 overcrowded.

247 To address the overcrowding issue, we introduced a competition mechanism. When two  
248 or more populations overcrowd in one area, they will compete with each other. We first  
249 merge all overcrowding populations in that area, then rank all individuals of the combined  
250 population according to the objective value, finally keep the best  $m$  individuals and remove  
251 the remaining. The overcrowding detection is performed every iteration, and the competition  
252 mechanism will be triggered whenever overcrowding populations are detected.

### 253 *Population Increase*

254 Increasing populations means increasing the diversity for exploring unexplored areas.  
255 However, to increase populations, we need to know when, how many, and where to generate  
256 new random solutions.

257 The moment to increase populations has a significant impact on the performance of  
258 an algorithm in dynamic environments (Li et al. 2015). Frequently increasing the diversity

259 causes the inefficiency issue in the exploitation of global optima, while infrequently increasing  
 260 the diversity causes the algorithm to fail to track the changes of the optima. In order to  
 261 solve this problem, we increase populations when all populations enter into a stable status  
 262 on the network indicated by the coverage ratio over all nodes, i.e., we increase populations  
 263 when the coverage ratio does not change over two successive iterations.

After the identification of the moment to increase populations, the next step is to determine how many populations to be increased. Inspired by (Li et al. 2016), we propose a feedback learning strategy based on historical data to estimate the number of populations to be increased. After the detection of the moment to increase populations, we record the number of populations ( $\tilde{k}(T)$ ) survived from the competition, then compare the reduced number with the previous increased number ( $\Delta k(T - 1)$ ), which is set to  $k(T = 0)/2$  initially. If the reduced number is less than the previous increased number, which is a positive feedback and means that new areas have been discovered, then the current increased number will be increased by one based on the previous increased number ( $\Delta k(T - 1)$ ); if the reduced number is greater than the previous increased number, which is a negative feedback and the current increased number will be decreased by one based on the previous increased number; otherwise, there is no change:

$$\Delta k(T) = \begin{cases} \Delta k(T - 1) + 1 & \text{if } \Delta k(T - 1) < k(T) - \tilde{k}(T) \\ \max(\Delta k(T - 1) - 1, 1) & \text{if } \Delta k(T - 1) > k(T) - \tilde{k}(T) \\ \Delta k(T - 1) & \text{if } \Delta k(T - 1) = k(T) - \tilde{k}(T) \end{cases} \quad (5)$$

264 Note that, there is at least one population to be increased in the negative feedback case to  
 265 make sure that finding new global optima is always possible.

266 Finally, we can generate random solutions to increase the population diversity. Different  
 267 from the traditional random immigrant scheme where new solutions are uniformly randomly  
 268 generated at all nodes without considering the distribution of the current and historical  
 269 solutions on the network, we generate new solutions at node  $i$  with probability  $p_i$  obtained

270 by Eq. (3). This way, infrequently visited nodes have large probabilities of being explored,  
271 which is very helpful for finding new global optima.

272 Note that, in order to respond to changes in dynamic environments, change detection is  
273 usually needed, or an algorithm is directly informed at the moment when a change occurs. For  
274 example, the algorithm (Liu et al. 2011) is informed once new data come, and mutation step  
275 lengths are reinitialized. In this paper, we do not need to detect changes. Here, to respond to  
276 changes, the population increase is determined only based on the current evolutionary status  
277 of the whole populations but not necessarily at the moment of a change occurring, i.e., the  
278 distribution of all solutions on the network does not changes means that the algorithm  
279 becomes converging and needs to be diversified to enhance the exploration capability.

## 280 RESULTS AND DISCUSSION

281 In this section, we conduct two groups of experiments to study the performance of the  
282 proposed algorithm. The first group of experiments aims to analyze the effect of the critical  
283 parameters on the performance of our algorithm, including the initial number of populations  
284  $k$  and the size of a single population  $m$ . The second group of experiments aims to compare  
285 the performance of our algorithm with several state-of-the-art evolutionary algorithms.

### 286 Experimental Setup

287 Our algorithm treats the water distribution network as a “black box”, the structure of the  
288 networks has little impact on the performance of the algorithm. When the scale of a WDS  
289 is quite large, the simulation time of evaluating a solution will become unaffordable, and the  
290 value range of the location will be increased sharply, resulting in a sharp increase in solution  
291 space. As a result, the algorithm performance may deteriorate. Then we take scales of the  
292 networks as main factor influencing the performance of algorithms.

293 Three networks were chosen with the scale from 97 nodes to 430 nodes, as shown in  
294 Figure 2. The configuration of each network is shown in Table 1, where the sensor nodes  
295 were set according to the literature in the way that they can cover as many nodes as possible

296 during the injection events. For each network, we set three different test cases, which are  
297 listed in Table 2, where the injection rate changes every 10 minutes.

298 In the experiments, the simulation duration was set to 24 hours, and observation data  
299 were collected from sensors every 10 minutes. Given the above configurations in Table 2,  
300 we assume that the range of  $[0h, 4h]$  for the start time and  $[5g, 30g]$  for the injection mass.  
301 Therefore, new solutions are randomly initialized within these ranges. To reduce the com-  
302 plexity of the problem, we assume the injection duration is known for all algorithms in this  
303 paper. All the results in this paper are averaged over 20 independent runs, and each test  
304 case was run for 200,000 objective evaluations.

305 Before the experiments, we conduct the hydraulic simulation for three water distribution  
306 network, we analyzed the water age of all nodes, and concluded that if the pollutants were  
307 injected at the water source, it can reach at each node during the simulation. We set sensors  
308 according to the locations provided by literature and our experience to make the coverage of  
309 the sensor as large as possible. Therefore, the occurrence of injection events can be detected  
310 within the simulation time even if some sensors are in low-flow zones.

311 We use a success rate and the prediction error to evaluate the performance of an algo-  
312 rithm. A successful run is a run where the true injection node is found, so the success rate is  
313 the number of successful runs over the total number of runs. Note that, the prediction error  
314 is averaged over all successful runs, not over the total number of runs in this paper.

### 315 **Parameter Sensitivity Analysis**

316 In this subsection, network 1 with configuration 1-3 in Table 2 was used to test the  
317 performance change of our algorithm with different combinations of  $k \in \{10, 20, 40\}$  and  
318  $m \in \{20, 50, 100\}$ , where each combination is listed in Table 3.

319 As shown in Table 4, the success rate is one regardless of the change in the size of a  
320 single population and the initial number of populations. The prediction error varies a little  
321 with different combinations. Figure 3 shows the change in the coverage rate and the number  
322 of populations on instance 1-3 of network 1 with a fixed single population size of  $m=50$ ,



323 where the initial number of populations is set to  $k=10/20/40$  from left to right. From the  
324 figure, it can be seen that the number of the diversity increase during the run is the same  
325 (i.e, five times) and the number of populations finally survived is maintained at all about  
326 nine. It indicates that the initial number of populations has no significant impact on the  
327 performance of the proposed algorithm. Due to the adaptation mechanism, the number  
328 of populations will be adjusted to an appropriate number for a specific problem. For the  
329 following experiments, the default initial number of populations is set to 20.

330 Figure 4 shows the change in the coverage rate and the number of populations on instance  
331 1-3 of network 1 with a fixed initial number of populations of 20, where the size of a single  
332 population is set to  $m=20/50/100$  from left to right. For the instance 1-3-4 with  $m=20$ ,  
333 compared with the instance 1-3-5 with  $m=50$ , the size of the overall populations is not enough  
334 to explore the whole search space. Therefore, the algorithm will frequently increase new  
335 populations to make up for the lack of the overall population size to improve its exploration  
336 capability. When  $m=100$ , the population size is enough for the problem, and the frequency  
337 of adding new population becomes low, which saves unnecessary computational overhead.  
338 Similarly, it can also be seen that the different sizes of a single population have no significant  
339 impact on the performance of the algorithm due to the diversity trigger mechanism. For a  
340 small size, more new populations will be added to achieve the best exploration capability  
341 and vice versa.

### 342 **Comparison with Other Algorithms**

343 In this subsection, three state-of-the-art simulation-optimization-based algorithms are  
344 chosen to compare with our algorithm, named AMP-CC(GL-SaDE) for short. The peer al-  
345 gorithms are ADOT-CC(GL-SaDE) (Liu et al. 2011), GD-ES (Zechman and Ranjithan 2009),  
346 and LRM-ADOT-CC(GL-SaDE) (Liu et al. 2012). Both ADOT-CC(GL-SaDE) and LRM-  
347 ADOT-CC(GL-SaDE) use an adaptive dynamic optimization technique based on multi-  
348 populations. The differences is that LRM-ADOT-CC(GL-SaDE) uses a logistic regression  
349 to predict the possible location of an injection event. GD-ES (Zechman and Ranjithan 2009)

350 uses evolution strategies (ESs) implemented with a tree-based encoding to represent variable-  
351 length decision variables. Note that, in order to compare the performance of the adaptive  
352 framework proposed in this paper with the one used in ADOT-CC(GL-SaDE) (Liu et al.  
353 2011) and LRM-ADOT-CC(GL-SaDE) (Liu et al. 2012), we use the same search method  
354 for each population (the cooperative co-evolutionary algorithm introduced in Section 3) for  
355 these three algorithms. The suggested parameter values were used for all the other three al-  
356 gorithms. Besides, the number of objective evaluations and consumed time for optimization  
357 are equivalent among our algorithm and three state-of-the-art algorithms.

### 358 *Comparison of the Success Rate and Prediction Error*

359 Table 5 shows the comparison of the success rate obtained by the four algorithms on  
360 each test instance where the best result of each instance is shown in bold font. It can be  
361 seen that AMP-CC(GL-SaDE) outperforms all the other three algorithms on five out of nine  
362 instances. AMP-CC(GL-SaDE) achieves a success rate of one on five out of nine instances  
363 and a minimum success rate of 0.9 on the other instances. For simple test instances with a  
364 short injection history, all the four algorithms can find the true location for all runs except  
365 GD-ES on instances of networks 2 and 3. However, when the injection profile increases, the  
366 performance of all the algorithms becomes worse. Compared with ADOT-CC(GL-SaDE),  
367 LRM-ADOT-CC(GL-SaDE) does improve the success rate due to the location prediction  
368 mechanism.

369 Table 6 presents the comparison of the prediction error obtained by all the four algorithms  
370 on all the test instances where the best result of each instance is shown in bold font. In  
371 each test case, the Wilcoxon rank sum test at a significant level of 0.05 is performed on  
372 the prediction error between our algorithm and other peer algorithms. The errors with  
373 suffixes +, -, or  $\approx$  indicate that the prediction errors obtained by other peer algorithms  
374 are significantly better than, significantly worse than, and statistically equivalent to our  
375 algorithm, respectively.

376 From Table 6, it can be seen that AMP-CC(GL-SaDE) outperforms all the other three

377 algorithms on all test instances. The performance of AMP-CC(GL-SaDE) is significantly bet-  
378 ter than the other three algorithms on instances 1-1, 2-1, 2-2, and 3-3. The error achieved  
379 by GD-ES is the worst among all the algorithms on small scale instances (networks 1 and 2).  
380 LRM-ADOT-CC(GL-SaDE) introduces a pre-screening mechanism based on a logical regres-  
381 sion model, which improves the performance on the small instances of networks 1 and 2, but  
382 not on the large instances of network 3. Due to the adaptation of the number of populations,  
383 AMP-CC(GL-SaDE) achieves much smaller errors than ADOT-based algorithms.

384 To test the impact of changing the total number of objective evaluations on the per-  
385 formance of the four algorithms, we run all the algorithms on instance 1-3 with different  
386 maximum numbers of objective evaluations. Figure 5 presents the comparison of the num-  
387 ber of populations obtained when the run finishes and the average best prediction error of  
388 each algorithm under different maximum numbers of evaluations on the test instance 1-3.  
389 From the comparison, we can have (1) AMP-CC(GL-SaDE) achieves the largest number of  
390 populations and it is always superior to other algorithms in terms of the prediction error and  
391 (2) the advantage of multi-population methods over single population methods can also be  
392 seen in the comparison, where all the errors obtained by the three multi-population methods  
393 decrease when the maximum number of objective evaluations increases.

#### 394 *Comparison of the Diversity Maintaining*

395 Figure 6 presents the comparison of the change in the coverage ratio and the number of  
396 populations for the four algorithms on instances 1-3 (sub-figures on the top) and 3-1 (sub-  
397 figures on the bottom). To some extent, the change in the coverage ratio during the runtime  
398 reflects the exploring capability of an algorithm, i.e., the ability to maintain the population  
399 diversity. Among the four algorithms, only GD-ES does not consider the population diversity.  
400 In Figure 6, the coverage ratio of GD-ES sharply drops to a low level even at the beginning  
401 of the run and maintains at that low level till the end of the run on both test instances. This  
402 may results in a premature convergence issue since the problem is highly multi-modal, which  
403 can explain the reason for the lower success rate of GD-ES than the other three algorithms.

404 The improvement of diversity is the key to improve the success rate of the algorithm, so  
405 how to increase diversity will directly affect the ability to find optimal solutions. ADOT-  
406 CC(GL-SaDE), LRM-ADOT-CC(GL-SaDE), and AMP-CC(GL-SaDE) all adopt the same  
407 search methods but use different multi-population frameworks. AMP-CC(GL-SaDE) uses  
408 the AMP framework proposed in this paper, and the other two use the ADOT framework  
409 (Liu et al. 2011). The essential difference between the two frameworks is the mechanism of  
410 increasing diversity. The ADOT framework uses a distance evaluation strategy to disperse  
411 individuals in the population to other regions, but it does not increase the coverage ratio  
412 as necessary. It is because ADOT does not increase individuals, but move them to other  
413 nodes already covered by existing solutions. This can be validated from the coverage ratio of  
414 ADOT-CC(GL-SaDE) and LRM-ADOT-CC(GL-SaDE) in Figure 6. Although this strategy  
415 increases the exploring ability to a certain extent, it does not expand the scope of exploration  
416 in essence, and its ability to search for new optima is not strong enough, which leads to the  
417 lower success rate in comparison with the AMP framework.

418 From the two curves of AMP-CC(GL-SaDE) on instance 1-3 in Figure 6 (the top right),  
419 it can be seen that when the coverage ratio remains for several iterations, the number of  
420 populations increases and the coverage ratio rises sharply to nearly one. At this moment,  
421 AMP-CC(GL-SaDE) expands the exploring area to the whole network. The AMP framework  
422 increases the population diversity at the global level, while the ADOT framework increases  
423 the population diversity at the local level within each population. Therefore, the exploring  
424 capability of the AMP framework is much stronger than that of the ADOT framework.

425 Moreover, in the AMP framework, new solutions are initialized in the areas, where no  
426 solution is covering, with a very large probability. During the runtime, the number of times  
427 for each node visited by solutions is recorded. The more times the node is visited, the more  
428 computing resources are spent at that node to optimize the injection history. However,  
429 when new solutions are added, more computing resources are placed at the nodes with a few  
430 visitors to find more global optima.

431 Different from the behavior of AMP-CC(GL-SaDE) on instance 1-3, the algorithm does  
432 not increase populations during the whole run on instance 3-1, i.e., the diversity increasing  
433 component is not triggered ( similar to the ADOT framework). The scale of the network 3 is  
434 much larger than that of network 1. Although the lowest level of the coverage ratio is similar  
435 in the two cases, the number of nodes covered on instance 3-1 is much larger than that on  
436 instance 1-3. This means that for the same given number of individuals, the population  
437 diversity on instance 3-1 is also much larger than that on instance 1-3. Therefore, given a  
438 limited evaluation budget, the algorithm spends more computing resources on exploiting the  
439 current area rather than exploring new areas and tries to improve its performance on the  
440 optimization of the historical injection profile. The comparison in the two scenarios shows  
441 that the AMP framework can adapt to problems with different scales.

#### 442 *Comparison of the Injection Profile*

443 Figure 7 shows the time-varying mean of contaminants concentrations observed at four  
444 detection points on instance 1-3, where the solid red curve refers to the actual observation  
445 data, the solid dark curve refers to the contaminants concentrations simulated by the best  
446 solution found by the algorithms, and the gray dashed curves are for the remaining solutions.  
447 It can be seen that the general trend of the dark solid curves are very close to the actual  
448 data, i.e., the optimal solutions found by the algorithms are sound. Compared with the  
449 other three algorithms, AMP-CC(GL-SaDE) finds more optimal solutions. The comparison  
450 further verifies that AMP-CC(GL-SaDE) has stronger exploring capability than the other  
451 three algorithms.

452 When we observe the change in the prediction error of the best solutions obtained by the  
453 four algorithms in Figure 8, all the three multi-population based algorithms can quickly locate  
454 the injection event in the beginning of the run except GD-ES. However, it is interesting to  
455 observe that the performance of the three algorithms deteriorates when the new observation  
456 data keep coming. The prediction errors of both ADOT-CC(GL-SaDE) and LRM-ADOT-  
457 CC(GL-SaDE) are even worse than that of GD-ES after the number of evaluations reaches

30,000. Among the four algorithms, AMP-CC(GL-SaDE) achieves the minimal error for most of the running time.

### Performance Investigation on Dynamic Contamination Sources

In this subsection, we identify dynamic contamination sources by our algorithm. To make sure that there is enough time for distributing the injected masses, the simulation duration was set to 48 hours, and observation data were collected from sensors every 10 minutes, other parameters of our algorithm were set as above. However, the location of the contamination source changes every six hours. Network 1 with four contamination sources change was used to test the performance by our algorithm. The injection rate of four sources was all set to 30,25,20,15,10,5,5,10,15,20,25,30 for simplicity. Considering that the current water quality of the water distribution network will be affected by the contamination sources in the previous stages, in our algorithm. Each simulation is from the beginning to the current time phase. In each stage, when a sensor detects that the contamination exceeds a certain threshold, the algorithm starts to optimize and search for the optimal location and injection rate of the pollution source in the current stage.

Table 7 shows the errors and success rates over 20 runs. The success rate of finding the real contamination source in each stage is 0.95, 1, 1 and 1. It can be seen that our algorithm also works well for dynamic contamination sources and can accurately find the real sources at each stage. The prediction error is shown in Figure 9. There are three peaks in the figure, because when the pollution source changes, the optimal solution of the existing population is no longer the global optimal solution, and the error will suddenly increase. However, the error quickly drops due to the parallel search ability of the proposed algorithm. Figure 10 shows the time-varying mean of contaminants concentrations observed at four detection points of one single run, where the solid red curve refers to the actual observation data, the solid dark curve refers to the contaminants concentrations simulated by the best solution found by the algorithm in terms of the error, and the gray dashed curves are for the remaining two best solutions. It can be seen that that there are four peaks during the runtime, which means

485 there are four different sources of pollution, and our algorithm can track the optimal solution  
486 well.

## 487 **CONCLUSIONS**

488 This paper proposes an adaptive multi-population framework to solve the contamination  
489 source identification problem in the water distribution system. The problem is defined as a  
490 dynamic bilevel optimization problem. To handle the real-time and non-uniqueness charac-  
491 teristics of the problem, we develop an adaptive mechanism to enhance the exploring ability  
492 of multi-population methods and a cooperative co-evolution strategy for the bilevel opti-  
493 mization problem. The AMP framework can automatically remove redundant populations  
494 and adds a proper number of populations at a proper moment, which makes it adaptable to  
495 different problems.

496 From the experimental results, we can draw the following two conclusions. Firstly, the  
497 multi-population based methods have advantages over single-population based algorithms.  
498 Secondly, by removing crowding populations in over-exploited areas and adding new popu-  
499 lations in unexplored areas, the AMP framework can find more candidate solutions than the  
500 ADOT framework. As a result, it significantly improves the success rate in finding the true  
501 optimal solution.

502 We want to pursue the following work in the future. Firstly, more uncertain factors  
503 should be considered during the simulation, e.g., network structures and the sensor locations.  
504 Secondly, multiple contamination sources should also be considered in a dynamic scenario.  
505 Thirdly, the simulation of large scale problems is very time-expensive, which is challenging  
506 to simulation-optimization based methods. Finally, the number and the location of sensors  
507 on the network is also an interesting topic.

## 508 **DATA AVAILABILITY**

509 Some or all data, models, or code generated or used during the study are available in a  
510 repository online in accordance with funder data retention policies.

511 The source code for all the involved algorithms in this paper will be released in OFEC,  
512 which is an open framework for evolutionary computation, at the link [https://github.](https://github.com/Changhe160/OFEC)  
513 [com/Changhe160/OFEC](https://github.com/Changhe160/OFEC).

## 514 ACKNOWLEDGMENTS

515 This work was supported in part by the National Natural Science Foundation of China  
516 under Grants 61673355, 61673331, and 62076226, in part by the Fundamental Research  
517 Funds for the Central Universities China University of Geosciences (Wuhan) under Grants  
518 CUG170603 and CUGGC02, in part by the Hubei Provincial Natural Science Foundation of  
519 China under Grant 2015CFA010, in part by the 111 project under Grant B17040, in part  
520 by the European Union’s Horizon 2020 research and innovation programme under grant  
521 agreement No. 739551 (KIOS CoE) and from the Government of the Republic of Cyprus  
522 through the Directorate General for European Programmes, Coordination and Development.

## 523 REFERENCES

- 524 Berry, J., Hart, W., Phillips, C., Uber, J., and Watson, J. (2006). “Sensor placement in  
525 municipal water networks with temporal integer programming models.” *Journal of Water*  
526 *Resources Planning & Management*, 132(4), p. 218–224.
- 527 Costa, D. M., Melo, L. F., and Martins, F. G. (2013). “Localization of contamination sources  
528 in drinking water distribution systems: A method based on successive positive readings of  
529 sensors.” *Water Resources Management*, 27(13), 4623–4635.
- 530 Cristo, C. D. and Leopardi, A. (2008). “Pollution source identification of accidental con-  
531 tamination in water distribution networks.” *Journal of Water Resources Planning and*  
532 *Management*, 134(2), 197–202.
- 533 Guan, J., Aral, M. M., Maslia, M. L., and Grayman, W. M. (2006). “Identification of contam-  
534 inant sources in water distribution systems using simulation-optimization method: Case  
535 study.” *Journal of Water Resources Planning and Management*, 132(4), 252–262.
- 536 Guneshwor, L., Eldho, T. I., and Kumar, A. V. (2018). “Identification of groundwater con-



537 tamination sources using meshfree rpcm simulation and particle swarm optimization.”  
538 *Water Resources Management*, 32(4), 1517–1538.

539 Hu, C., Zhao, J., Yan, X., Zeng, D., and Guo, S. (2015). “A map reduce based parallel niche  
540 genetic algorithm for contaminant source identification in water distribution network.” *Ad  
541 Hoc Networks*, 35(DEC.), 116–126.

542 Huang, J. J. and Mcbean, E. A. (2009). “Data mining to identify contaminant event locations  
543 in water distribution systems.” *Journal of Water Resources Planning and Management*,  
544 135(6), 466–474.

545 Laird, C. D., Biegler, L. T., Waanders, B. G. V. B., and Bartlett, R. A. (2005). “Contam-  
546 ination source determination for water networks.” *Journal of Water Resources Planning  
547 and Management*, 131(2), 125–134.

548 Li, C., Nguyen, T. T., Yang, M., Mavrovouniotis, M., and Yang, S. (2016). “An adaptive  
549 multipopulation framework for locating and tracking multiple optima.” *IEEE Transactions  
550 on Evolutionary Computation*, 20(4), 590–605.

551 Li, C., Nguyen, T. T., Yang, M., Yang, S., and Zeng, S. (2015). “Multi-population methods in  
552 unconstrained continuous dynamic environments: The challenges.” *Information Sciences*,  
553 296, 95–118.

554 Li, C. and Yang, S. (2012). “A general framework of multipopulation methods with clustering  
555 in undetectable dynamic environments.” *IEEE Transactions on Evolutionary Computa-  
556 tion*, 16(4), 556–577.

557 Liu, L. and Ranjithan, S. R. (2010). “An adaptive optimization technique for dynamic envi-  
558 ronments.” *Engineering Applications of Artificial Intelligence*, 23(5), 772–779.

559 Liu, L., Ranjithan, S. R., and Mahinthakumar, G. (2011). “Contamination source identifi-  
560 cation in water distribution systems using an adaptive dynamic optimization procedure.”  
561 *Journal of Water Resources Planning and Management*, 137(2), 183–192.

562 Liu, L., Zechman, E. M., Brill, Jr, E. D., Mahinthakumar, G., Ranjithan, S., and Uber, J.  
563 (2008). “Adaptive contamination source identification in water distribution systems using

564 an evolutionary algorithm-based dynamic optimization procedure.” *Water Distribution*  
565 *Systems Analysis Symposium 2006*, 1–9.

566 Liu, L., Zechman, E. M., Mahinthakumar, G., and Ranji Ranjithan, S. (2012). “Identifying  
567 contaminant sources for water distribution systems using a hybrid method.” *Civil Engi-*  
568 *neering and Environmental Systems*, 29(2), 123–136.

569 Olikier, N. and Ostfeld, A. (2014). “A coupled classification - evolutionary optimization model  
570 for contamination event detection in water distribution systems.” *Water Research*, 51, 234–  
571 245.

572 Ostfeld, A. and Salomons, E. (2004). “Optimal layout of early warning detection stations for  
573 water distribution systems security.” *Journal of Water Resources Planning and Manage-*  
574 *ment*, 130(5), 377–385.

575 Ostfeld, A. and Salomons, E. (2005). “Optimal early warning monitoring system layout  
576 for water networks security: inclusion of sensors sensitivities and response delays.” *Civil*  
577 *Engineering and Environmental Systems*, 22(3), 151–169.

578 Perelman, L. and Ostfeld, A. (2013). “Bayesian networks for source intrusion detection.”  
579 *Journal of Water Resources Planning and Management*, 139(4), 426–432.

580 Potter, M. A. and De Jong, K. A. (1994). “A cooperative coevolutionary approach to function  
581 optimization.” *Parallel Problem Solving from Nature (PPSN)*, 249–257.

582 Preis, A. and Ostfeld, A. (2006). “Contamination source identification in water systems: A  
583 hybrid model trees-linear programming scheme.” *Journal of Water Resources Planning*  
584 *and Management*, 132(4), 263–273.

585 Preis, A. and Ostfeld, A. (2008). “Genetic algorithm for contaminant source characterization  
586 using imperfect sensors.” *Civil Engineering and Environmental Systems*, 25(1), 29–39.

587 Propato, M. (2006). “Contamination warning in water networks: General mixed-integer linear  
588 models for sensor location design.” *Journal of Water Resources Planning & Management*,  
589 132(4), p. 225–233.

590 Qin, A. K., Huang, V. L., and Suganthan, P. N. (2009). “Differential evolution algorithm

591 with strategy adaptation for global numerical optimization.” *IEEE Transactions on Evo-*  
592 *lutionary Computation*, 13(2), 398–417.

593 Rossman, L. A. (2000). “Epanet 2 users’ manual.” *Report no.*, U. S. Environmental Protection  
594 Agency.

595 Sankary, N. and Ostfeld, A. (2018). “Multiobjective optimization of inline mobile and fixed  
596 wireless sensor networks under conditions of demand uncertainty.” *Journal of Water Re-*  
597 *sources Planning and Management*, 144(8), 04018043.

598 Seth, A., Klise, K. A., Siirola, J. D., Haxton, T., and Laird, C. D. (2016). “Testing contam-  
599 ination source identification methods for water distribution networks.” *Journal of Water*  
600 *Resources Planning & Management*, 142(4), 04016001.1–04016001.11.

601 Shang, F., Uber, J. G., and Polycarpou, M. M. (2002). “Particle backtracking algorithm  
602 for water distribution system analysis.” *Journal of Environmental Engineering*, 128(5),  
603 441–450.

604 Sreepathi, S., Mahinthakumar, K., Zechman, E., Ranjithan, R., Brill, D., Ma, X., and  
605 Von Laszewski, G. (2007). “Cyberinfrastructure for contamination source characteriza-  
606 tion in water distribution systems.” *International Conference on Computational Science*,  
607 Springer, 1058–1065.

608 Storn, R. and Price, K. (1997). “Differential evolution—a simple and efficient heuristic for  
609 global optimization over continuous spaces.” *Journal of global optimization*, 11(4), 341–  
610 359.

611 Taormina, R. and Galelli, S. (2018). “Deep-learning approach to the detection and localiza-  
612 tion of cyber-physical attacks on water distribution systems.” *Journal of Water Resources*  
613 *Planning and Management*, 144(10), 04018065.

614 Xia, Y. and Li, C. (2016). “Memory-based statistical learning for the travelling salesman  
615 problem.” *2016 IEEE Congress on Evolutionary Computation (CEC)*, IEEE, 2935–2941.

616 Xin, K., Sheng, X., Tao, T., and Xiang, N. (2013). “Contamination source identification  
617 in water distribution networks based on negative gradient method.” *Journal of Tongji*

618 *University*, 41(1), 116–120.

619 Yan, X., Zhao, J., Hu, C., and Wu, Q. (2016). “Contaminant source identification in water  
620 distribution network based on hybrid encoding.” *Journal of Computational Methods in  
621 Sciences and Engineering*, 16(2), 379–390.

622 Yang, M., Omidvar, M., Li, C., Li, X., Cai, Z., Kazimipour, B., and Yao, X. (2017). “Efficient  
623 resource allocation in cooperative co-evolution for large-scale global optimization.” *IEEE  
624 Transactions on Evolutionary Computation*, 21(4), 493–505.

625 Yang, S. and Li, C. (2010). “A clustering particle swarm optimizer for locating and tracking  
626 multiple optima in dynamic environments.” *IEEE Transactions on Evolutionary Compu-  
627 tation*, 14(6), 959–974.

628 Yang, X., Boccelli, D. L., and De Sanctis, A. E. (2011). “A bayesian approach for probabilistic  
629 contamination source identification.” *World Environmental and Water Resources Congress  
630 2011: Bearing Knowledge for Sustainability*, American Society of Civil Engineers, 304–313.

631 Zechman, E. M. and Ranjithan, S. R. (2009). “Evolutionary computation-based methods  
632 for characterizing contaminant sources in a water distribution system.” *Journal of Water  
633 Resources Planning and Management*, 135(5), 334–343.

634 Zierolf, M. L., Polycarpou, M. M., and Uber, J. G. (1998). “Development and autocalibration  
635 of an input-output model of chlorine transport in drinking water distribution systems.”  
636 *IEEE transactions on control systems technology*, 6(4), 543–553.

637 **List of Tables**

638	1	Network configurations . . . . .	30
639	2	Configurations for nine test instances . . . . .	31
640	3	Combinations of the initial number of populations ( $k$ ) and the population size	
641		( $m$ ) for test instance 1-3 in Table 2 . . . . .	32
642	4	Success rates and prediction errors of different combinations of $k$ and $m$ on	
643		network 1 with configuration 1-3 . . . . .	33
644	5	Success rate of all the four algorithms in all the test cases . . . . .	34
645	6	Prediction error and standard deviation of all the four algorithms in all the	
646		test cases . . . . .	35
647	7	Results of dynamic sources over 20 runs on network 1 . . . . .	36

**TABLE 1. Network configurations**

Network	# of nodes	# of sensors	Sensor location
1	97	4	113, 147, 211, 120
2	279	12	J-124, J-202, J-204, J-196, J-122, J-267, J-115, J-197, J-14, J-55, J-3, J-58
3	430	16	J-56, J-321, J-296, J-11, J-258, J-209, J-118, J-345, J-112, J-121, J-69, J-171, J-200, J-6, J-342, J-229

**TABLE 2. Configurations for nine test instances**

Instance	Location	Start time	Duration (min)	Injection rate	
Network 1	1-1	113	0:00	60	5,10,15,20,15,10
	1-2	157	2:00	120	30,25,20,15,10,5,5,10,15,20,25,30
	1-3	267	4:00	240	30,5,30,5, . . . , 30,5,30,5
Network 2	2-1	J-196	0:00	60	5,10,15,20,15,10
	2-2	J-124	2:00	120	30,25,20,15,10,5,5,10,15,20,25,30
	2-3	J-146	4:00	240	30,5,30,5, . . . , 30,5,30,5
Network 3	3-1	J-37	0:00	60	5,10,15,20,15,10
	3-2	J-242	2:00	120	30,25,20,15,10,5,5,10,15,20,25,30
	3-3	J-56	4:00	240	30,5,30,5, . . . , 30,5,30,5

**TABLE 3. Combinations of the initial number of populations ( $k$ ) and the population size ( $m$ ) for test instance 1-3 in Table 2**

Instance	1-3-1	1-3-2	1-3-3	1-3-4	1-3-5	1-3-6	1-3-7	1-3-8	1-3-9
$k$	10	10	10	20	20	20	40	40	40
$m$	20	50	100	20	50	100	20	50	100



**TABLE 4. Success rates and prediction errors of different combinations of  $k$  and  $m$  on network 1 with configuration 1-3**

Instance	1-3-1	1-3-2	1-3-3	1-3-4	1-3-5	1-3-6	1-3-7	1-3-8	1-3-9
Success rate	1	1	1	1	1	1	1	1	1
Error	1.55E+01	1.33E+01	1.36E+01	1.31E+01	1.30E+01	1.38E+01	1.55E+01	1.40E+01	1.41E+01

**TABLE 5. Success rate of all the four algorithms in all the test cases**

Algorithm	1-1	1-2	1-3	2-1	2-2	2-3	3-1	3-2	3-3
GD-ES	<b>1</b>	0.1	0.1	0.7	0.8	0.6	0.8	0.7	0.8
ADOT-CC(GL-SaDE)	<b>1</b>	0.65	0.5	<b>1</b>	<b>1</b>	0.7	<b>1</b>	0.9	0.4
LRM-ADOT-CC(GL-SaDE)	<b>1</b>	0.65	0.7	<b>1</b>	<b>1</b>	0.3	<b>1</b>	0.7	<b>1</b>
AMP-CC(GL-SaDE)	<b>1</b>	<b>0.95</b>	<b>1</b>	<b>1</b>	<b>1</b>	<b>0.9</b>	<b>1</b>	<b>0.9</b>	<b>0.9</b>

**TABLE 6. Prediction error and standard deviation of all the four algorithms in all the test cases**

Instance	GD-ES	ADOT-CC(GL-SaDE)	LRM-ADOT-CC(GL-SaDE)	AMP-CC(GL-SaDE)
1-1	7.8E+00±2.4E+00 <sup>-</sup>	5.4E-02±2.3E-03 <sup>-</sup>	2.7E-02±4.5E-03 <sup>-</sup>	<b>0</b>
1-2	6.4E+00±0≈	3.6E+00±1.2E+00≈	3.5E+00±1.7E+00≈	<b>2.6E+00±1.9E+00</b>
1-3	<b>1.3E+01±0≈</b>	1.5E+01±3.2E+00≈	1.5E+01±4.2E+00≈	<b>1.3E+01±3.0E+00</b>
2-1	6.6E+00±1.5E+00 <sup>-</sup>	8.7E-03±2.8E-04 <sup>-</sup>	2.3E-02±3.3E-03 <sup>-</sup>	<b>0</b>
2-2	9.3E+00±9.5E-01 <sup>-</sup>	3.1E-02±7.5E-03 <sup>-</sup>	6.2E-02±6.1E-03 <sup>-</sup>	<b>0</b>
2-3	1.5E+01±1.4E+00≈	1.6E+01±1.7E+00≈	1.5E+01±4.2E+00≈	<b>1.4E+01±1.3E+00</b>
3-1	7.7E+00±2.9E+00≈	6.2E+00±2.2E+00≈	8.6E+00±1.9E+00≈	<b>4.5E+00±2.3E+00</b>
3-2	8.5E+00±2.3E+00≈	7.5E+00±3.8E+00≈	1.1E+01±4.3E+00≈	<b>7.2E+00±2.6E+00</b>
3-3	1.2E+01±1.7E+00 <sup>-</sup>	1.3E-01±1.1E-02 <sup>-</sup>	2.1E-01±1.8E-02 <sup>-</sup>	<b>5.4E-02±2.1E-03</b>

**TABLE 7. Results of dynamic sources over 20 runs on network 1**

Run ID	Location	Error	Standard deviation
1	193 120 205 113	3.48E-02	2.94E+00
2	193 120 205 113	8.67E-02	4.80E+00
3	193 120 205 113	3.75E-02	4.63E+00
4	193 120 205 113	2.51E-02	4.46E+00
5	193 120 205 113	2.70E-02	2.70E+00
6	193 120 205 113	5.00E-02	1.85E+00
7	273 120 205 113	1.50E-01	8.26E+00
8	193 120 205 113	3.29E-02	2.89E+00
9	193 120 205 113	3.74E-02	4.02E+00
10	193 120 205 113	1.97E-02	3.17E+00
11	193 120 205 113	1.15E-02	3.31E+00
12	173 120 205 113	7.90E-02	6.37E+00
13	193 120 205 113	8.35E-02	2.36E+00
14	193 120 205 113	1.70E-02	4.37E+00
15	193 120 205 113	1.72E-02	4.43E+00
16	193 120 205 113	3.52E-02	5.75E+00
17	193 120 205 113	2.42E-02	3.36E+00
18	193 120 205 113	4.78E-02	3.54E+00
19	193 120 205 113	2.01E-02	2.28E+00
20	193 120 205 113	3.07E-02	1.80E+00

648 **List of Figures**

649	1	Framework of the adaptive multi-population method . . . . .	38
650	2	The picture of three network with 97/279/430 nodes . . . . .	39
651	3	The change in the number of populations and the coverage ratio on instances	
652		1-3-2/5/8 . . . . .	40
653	4	The change in the number of populations and the coverage ratio on instances	
654		1-3-4/5/6 . . . . .	41
655	5	The comparison of the number of populations (left) and the prediction error	
656		(right) obtained by the four algorithms, where a single population is used in	
657		GE-ES . . . . .	42
658	6	Comparison of the change in the coverage ratio and the number of populations	
659		for the four algorithms on instances 1-3 (top) and 3-1 (bottom) . . . . .	43
660	7	Solutions found by the four algorithm on instance 1-3 . . . . .	44
661	8	Comparison of the change in the prediction error on instance 1-3 . . . . .	45
662	9	The prediction error on case of dynamic contamination sources . . . . .	46
663	10	Sensor concentration in the case of dynamic contamination sources . . . . .	47

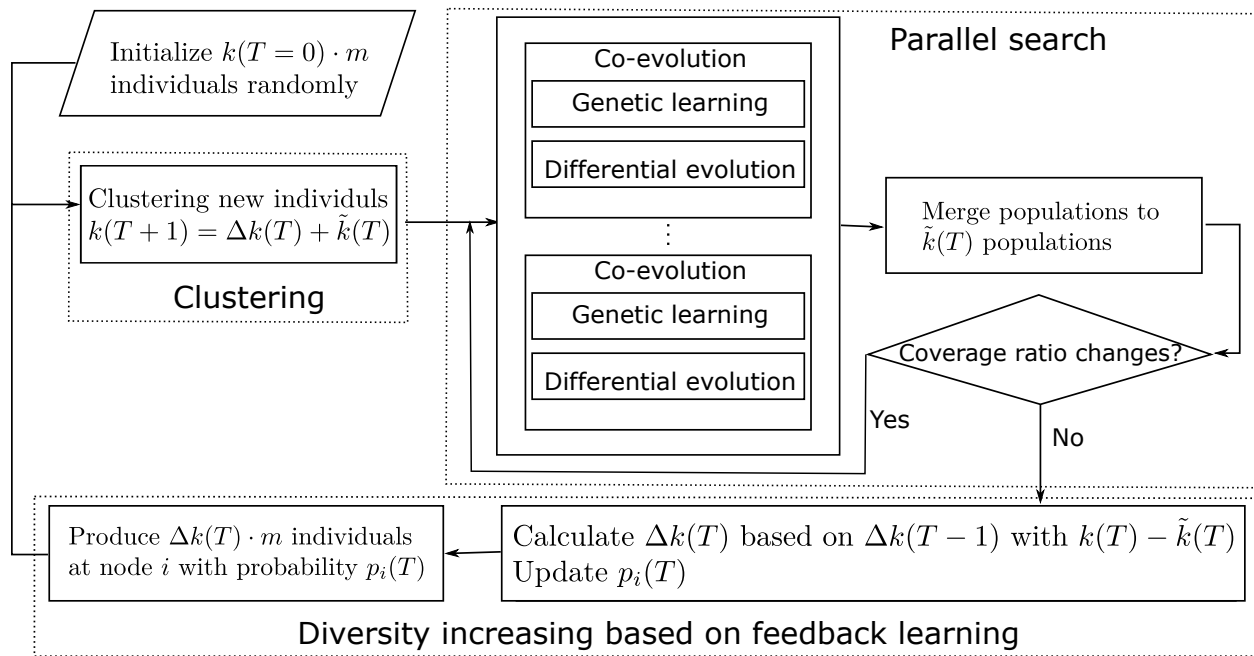


FIG. 1. Framework of the adaptive multi-population method

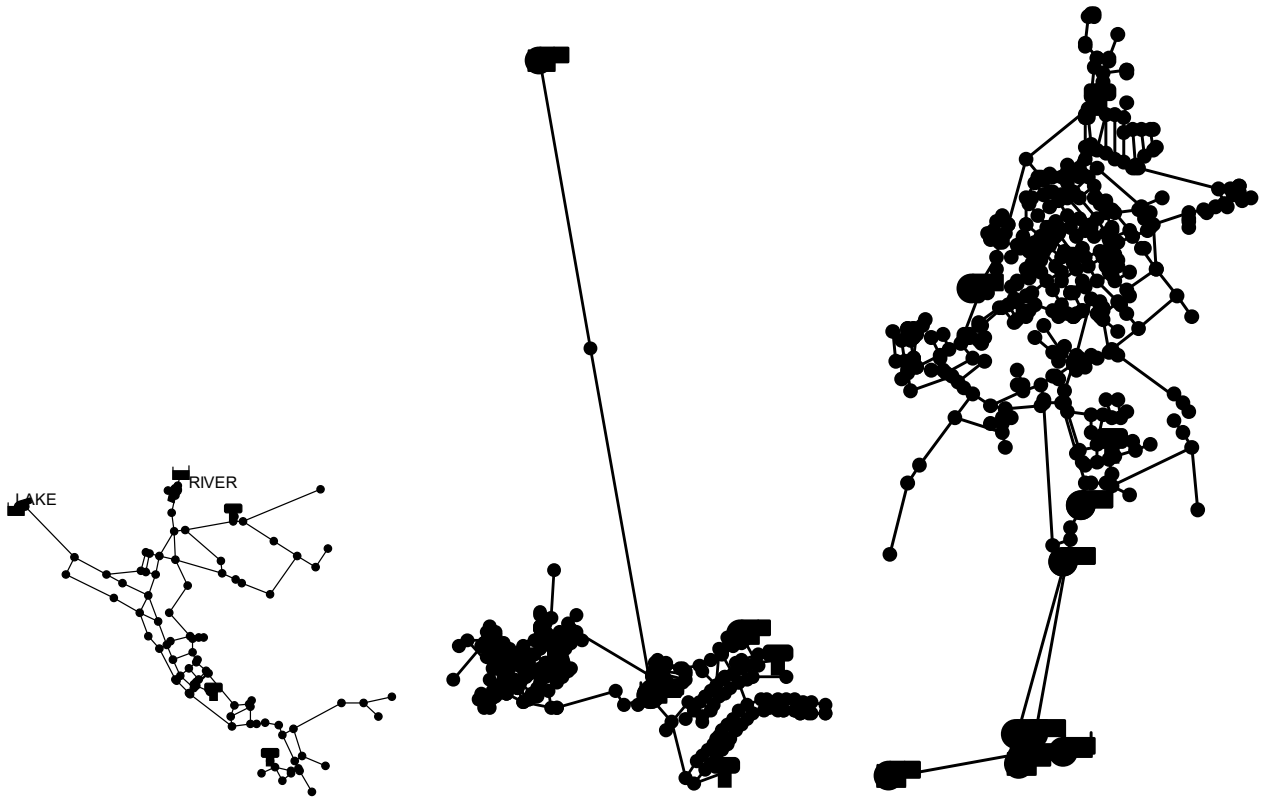
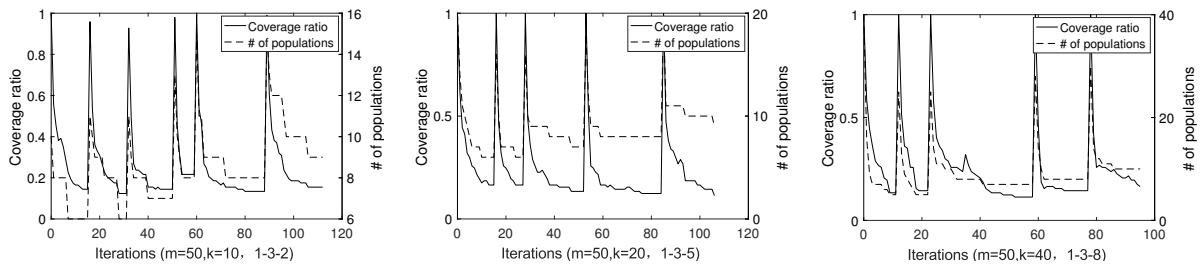
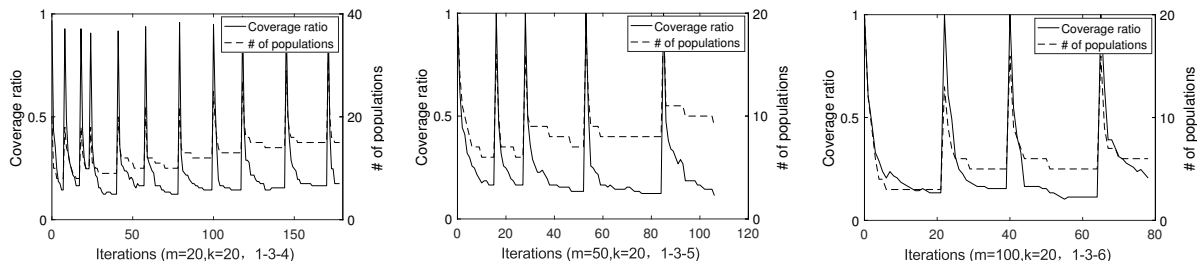


FIG. 2. The picture of three network with 97/279/430 nodes



**FIG. 3.** The change in the number of populations and the coverage ratio on instances 1-3-2/5/8





**FIG. 4.** The change in the number of populations and the coverage ratio on instances 1-3-4/5/6

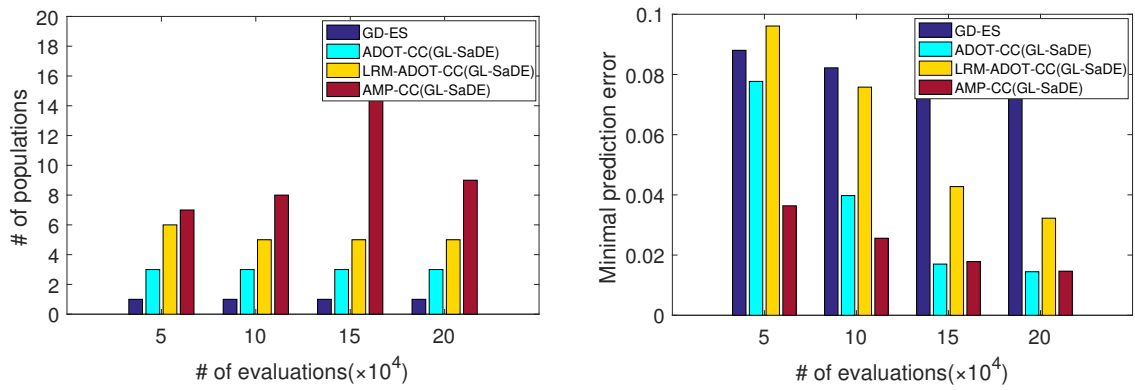


FIG. 5. The comparison of the number of populations (left) and the prediction error (right) obtained by the four algorithms, where a single population is used in GE-ES

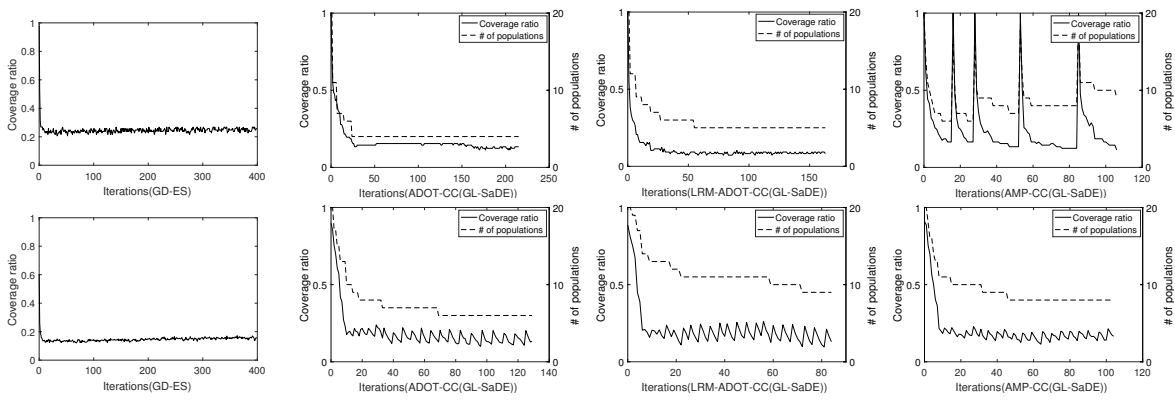
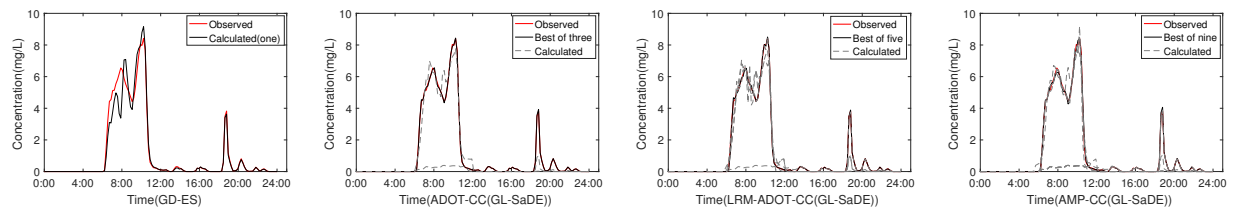


FIG. 6. Comparison of the change in the coverage ratio and the number of populations for the four algorithms on instances 1-3 (top) and 3-1 (bottom)



**FIG. 7. Solutions found by the four algorithm on instance 1-3**

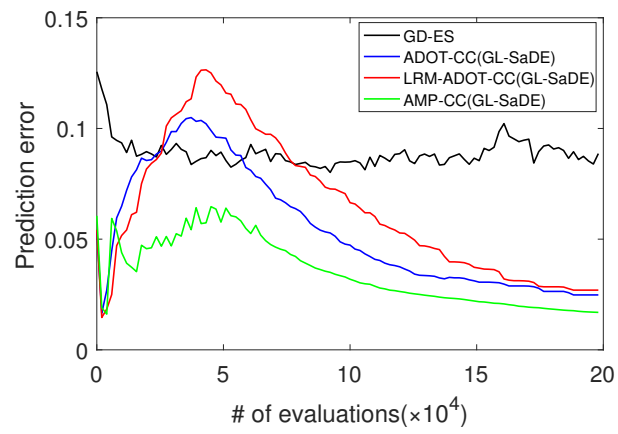
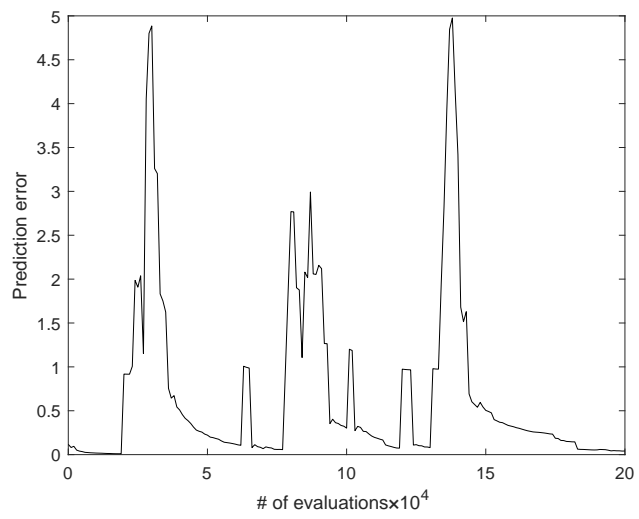


FIG. 8. Comparison of the change in the prediction error on instance 1-3



**FIG. 9.** The prediction error on case of dynamic contamination sources

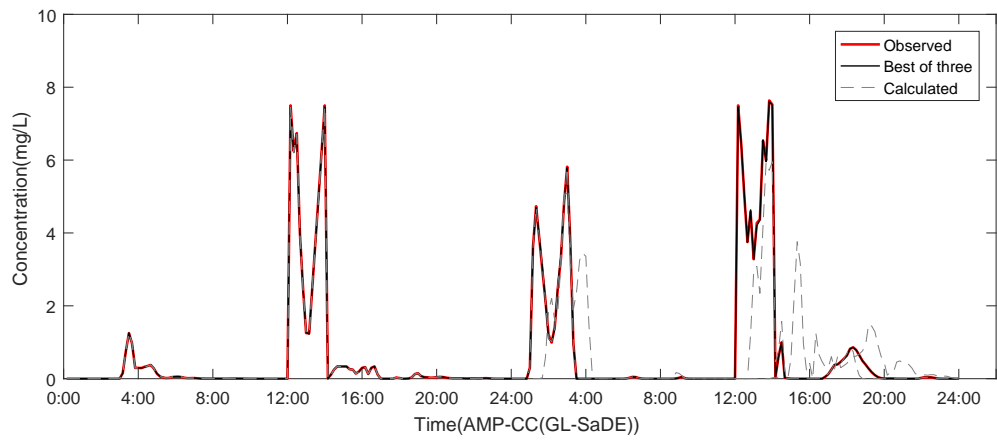


FIG. 10. Sensor concentration in the case of dynamic contamination sources